BA-92-80

Physics Modelling of Cosmic Ray Experiments

T. K. Gaisser
Bartol Research Institute
University of Delaware, Newark DE 19716

Talk Presented at the 1992 Vulcano Workshop, "Frontier Objects in Astrophysics and Particle Physics", December 2, 1992.

PHYSICS MODELLING OF COSMIC RAY EXPERIMENTS

T.K. Gaisser[1]

Bartol Research Institute
University of Delaware
Newark DE 19716

ABSTRACT

In this talk I compare several models of interactions of nuclei and hadrons and discuss their consequences for interpretation of air shower experiments above 100 TeV. The goal is to understand the "knee" of the cosmic ray spectrum.

1 Introduction

The intensity of primary cosmic rays above 100 TeV is about one particle per m^2sr hour. It decreases by a factor of about 50 for each decade increase in energy. As a consequence, it is necessary to use ground-based air shower experiments to achieve large enough exposure factors to study the cosmic radiation in the energy region $E \gg 100$ TeV. The indirect nature of the experiments means that modelling of the atmospheric cascades is essential for interpretation of the measurements to obtain information about primary composition and spectrum.

It has been known for many years [1] that there is a feature in the cosmic ray spectrum between 10^{15} and 10^{16} eV (the *knee*) which could be a key for understanding the origin of the high energy cosmic radiation. More recently, a theoretical picture for the origin of cosmic rays has developed that involves first order Fermi acceleration at shocks driven by supernova explosions. The power available in kinetic energy of supernova remnants ($\sim 10^{51}$ ergs per supernova in the galaxy) is well-matched to the power required to maintain the cosmic radiation ($\sim 5 \times 10^{40}$ erg/s or 5×10^{49} erg every 30 years).[2] Moreover, first order diffusive acceleration at strong shocks [3, 4, 5, 6] naturally gives a spectral index close to what is required to explain the observed cosmic ray spectrum.

The limitation of this picture is that there is an upper limit to the energy per particle that can be achieved, due to the finite lifetime of the process. It is given by

$$E_{\max} \sim \frac{u}{c} e Z B L, \tag{1}$$

[1]Work supported in part by the U.S. Department of Energy (Grant DE-FG02-91ER40626) and in part by NASA (Grant NAG-5-1573).

where u is the shock velocity, eZ the particle's charge, B the ambient magnetic field and $L = uT$, where T is the characteristic time during which the acceleration process is maximally effective. For a supernova expanding into the interstellar medium, the limit is $E_{\rm max}/Z \sim 100$ TeV.[7] The problem of how to account for the more energetic cosmic rays is one of great current interest.

One line of argument is that the supernova mechanism itself extends beyond the limit of $\sim$ 100 TeV. Considerations of magnetic field geometry[8], enhanced magnetic field due to the stellar wind of the precursor giant star[9], acceleration in supernova groups of particles pre-accelerated by a single supernova[10] and reacceleration to higher energy by a galactic wind[11] have all been suggested. Another possibility is simply that there is a new class of sources[12, 13], such as pulsars, for the particles with $E \gg 100$ TeV. It has long been thought that the very highest energy cosmic rays ($E > 10^{19}$ eV) are probably of extragalactic origin. Recently Protheroe & Szabo [14] have suggested that a significant fraction (all?) of the cosmic rays around the knee of the spectrum may of extragalactic origin, accelerated in accretion shocks around massive black holes at the centers of active galactic nuclei.

A good knowledge of the relative abundances of nuclei and of their energy spectra in the region of the knee can help to distinguish among these various possibilities. For example, any AGN contribution would consist entirely of protons, all nuclei having been broken down by photodisintegration in the vicinity of the source. If instead most cosmic rays in this energy region originated from the interior of supernova ejecta, one would expect a large fraction of heavy nuclei. In the reacceleration (or extended supernova acceleration) models, there would be a gradual increase of the fraction of heavy nuclei (classified by energy per nucleus) through the energy region of the knee of the spectrum. As in the original suggestion of Peters[1], this is a consequence of the assumed dependence of the spectrum on rigidity in a region of steepening.

2 Current Status

Fig. 1[15] is a composite energy spectrum which shows both direct measurements and air shower data. Because of its steepness, it is customary to display the differential spectrum multiplied by the energy raised to a power. This has the advantage of allowing an expanded vertical scale at the price of magnifying any systematic uncertainty in the energy calibration. For comparison with the air shower experiments, all data are plotted as a function of total energy per nucleus. The direct measurements of the all-particle spectrum in the satellite experiment [19] of Grigorov *et al.*[2] are consistent with the air shower measurements up to $\sim 3\times10^{15}$ eV. In addition, the sum of the individual spectra from JACEE [18] is consistent with the all-particle spectrum up to $\sim 3\times10^{14}$ eV. Thus there is consistency between direct measurements and air shower determinations of the spectrum up to $\sim 10^{15}$ eV.

A standard approach to analysis of air shower experiments is to assume a specific model spectrum and use it as input to a coscade calculaton, the result of which is

[2]According to Ellsworth *et al.* [22], the separation between protons and other nuclei in this experiment is flawed, but the all-particle spectrum appears valid.

compared to data of the experiment. Results of several model spectra with different compositions are then compared to select the one that best reproduces the data. It is important with this approach to ensure that any trial model is consistent with all existing data. In the region above 3×10^{15} eV, where only air shower data exist, the all particle spectrum is ambiguous to the extent that the conversion from measured shower size to primary energy depends on composition.[23] Thus, a more correct procedure in this case would be to compute the size spectrum for each assumed composition model and attempt simultaneously to fit, for example, coincident multiple muons and measured size spectrum.

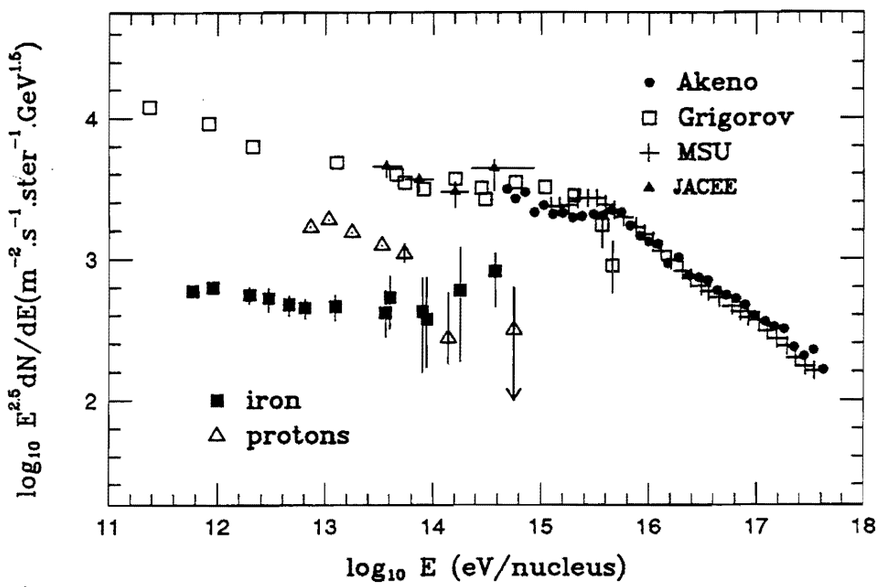

Figure 1. Summary of the all-particle spectrum. Data from two air shower experiments are shown, Akeno [16] and Moscow State University [17]. The four points with horizontal and vertical error bars are from JACEE [18], and the open boxes are from the Proton 4 experiment [19]. The proton spectrum [18] and iron spectrum [20, 21, 18] are shown for comparison.

Typical examples of trial spectra are those used by the NUSEX group [24] as the starting point for analysis of their data. They are "p-poor"[25]; "Maryland"[26]; "Constant Mass Composition"[27]; and "Linsley"[13]. The all particle spectra differ by as much as a factor of two above 10^{16} eV. This energy is well above the range of direct measurements, so the normalization cannot be checked directly; however, the model with the largest fraction of protons also has the highest intensity, which is likely to be in conflict with the observed rapid attenuation of the size spectrum.[16] Some of the models also appear to be inconsistent with direct measurements of iron and protons shown in Fig. 1.

The difficulty of reaching a definite conclusion about composition from a limited set of air shower data is apparent from the rather different conclusions reached by differ-

ent kinds of experiment. For example, simple anaylses of deep underground coincident multiple muons suggest a light composition in the region of the knee of the spectrum [28, 29, 30]. In contrast, the analysis of correlations between shower size and low energy muons by Erlykin *et al.* [31, 32] suggests an increasing fraction of heavy nuclei through the knee region. A challenge is to find a unique interpretation of a wide range of air shower data that is consistent at the low energy end ($\sim 10^{14}$ eV) with direct measurements and consistent with all air shower data at higher energies.

3 Interaction Models

The cascade calculations needed to link primary spectrum to ground level air shower data depend on two aspects of interaction models: treatment of nuclear projectiles and properties of high energy hadronic interactions. Here I will discuss the effects of interaction models on cascade development in the context of high energy muons in air showers. The energy region of interest includes the region of the knee of the spectrum and extends up to 10^{17} eV for high multiplicity events observed deep underground. A discussion of the role of interaction models in analysis of Fly's Eye data at significantly higher energy ($\sim 10^{18}$ eV or $\sqrt{s} \sim 40$ TeV) is discussed elsewhere.[33, 34]

3.1 Nucleus-nucleus collisions

The superposition model treats interactions in the atmosphere of nuclei of total energy E_0 and mass number A as A independent interactions of nucleons with energy E_0/A. This approximation omits correlations which may be important in some contexts. A central collision is characterized by a large number of wounded nucleons. Thus, an event in which the first interaction of a heavy cosmic ray projectile is central will produce a large number of secondary particles high in the atmosphere. Such showers will reach shower maximum earlier than average. In addition they will be characterized by a larger than average number of high energy muons because the low density at high altitude favors pion decay relative to pion interaction. In contrast, if the first few interactions happen to be peripheral collisions, the shower will penetrate deeper than average and produce a relatively small number of high energy muons. Note that the correlation between altitude of production and muon multiplicity will induce a correlation between multiplicity and separation of muons in an event.

A model which includes a realistic treatment of fluctuations in the framework of the Glauber multiple scattering model is described by Engel *et al.*.[35] In a simplified form (which neglects correlations between projectile nucleus and target air nucleus) this model can be used directly with a cascade code like HEMAS[36]. This cascade code treats a nuclear projectile as a succession of nucleon-induced showers with the location of the first inelastic interaction of each constituent nucleon specified by the nuclear model.[3] A still more realistic representation of nuclear interactions requires a cascade

[3]The non-superposition model included in the current HEMAS code is superceded by the fragmentation model of Ref. [35].

Table 1: Four interaction models.

	NIM85	TARGET	HEMAS	SIBYLL
Nuclear target effect	N	Y	Y	Y
Seagull effect	Y	Y	Y	Y
Increasing $\langle p_T \rangle$	N	Y	Y	Y
Rising rapidity plateau	N	Y	Y	Y
Tuned mult. distribution	N	N	Y	N
Minijets	N	N	N	Y
Beam-target correlation	N	N	N	Y
Beam-central correlation	N	N	N	Y

code which treats each type of nucleus and nuclear fragment as a particle on the same basis with hadrons and nucleons inside the cascade.

3.2 Hadronic interactions

3.2.1 Cross section

The $\bar{p}p$ cross section is measured up to $\sqrt{s} = 1.8$ TeV, equivalent to 1.7×10^{15} eV lab energy. The main source of uncertainty in cross section relevant to underground muons is therefore the conversion from $\bar{p}p$ to p-nucleus, π-nucleus and K-nucleus cross sections. Fortunately, production of high energy muons is relatively insensitive to uncertainties in cross section. If one increases or decreases both the proton and the pion interaction lengths (i.e. decrease or increase both cross sections relative to a standard) there is only a second order change in muon number and also in separation distribution. This is because there are two compensating effects. Increasing the proton interaction length makes the showers develop in a more dense part of the atmosphere where it is more difficult for pions to decay. However, increasing the pion interaction length gives the produced pions a longer pathlength in which to decay. For example, a 10% increase in both pion and nucleon interaction lengths changes the lateral spread and the mean number of muons by less than 2 or 3 per cent.

3.2.2 Inclusive cross sections

For illustration, I discuss four different event generators which correspond to somewhat different models of particle production in interactions of hadrons with nuclei in the atmosphere. The properties of the models are summarized in Table 1.

NIM85. This is a pure scaling model that uses Hillas' splitting algorithm [37] to select energies of secondary particles. It is very simple and very fast. The only correlations are imposed by energy-momentum conservation in conjunction with a broad leading particle distribution. This feature leads to large fluctuations from event to event in the amount of energy available for production of pions and kaons. The parameters

Table 2: Charged multiplicity in forward cm hemisphere

$E_{\rm lab}$(TeV	NIM85	TARGET	HEMAS	SIBYLL
1	5.8	6.8	5.5	5.3
10	8.7	11.1	9.8	9.9
100	11.6	16.7	15.0	17.3
1000	14.6	23.3	22.1	28.4

of Hillas' original model were chosen to fit fixed target data below 100 GeV lab energy. This interaction model was used for the parametrizations of deep underground muons published in Ref. [38]

TARGET. This model is a phenomenological fit to fixed target data on hadron-nucleus collisions. This interaction model has been used to calculate atmospheric neutrinos.[39] Known energy-dependent features, such as increase of mean p_T and rise of the central rapidity plateau are put in by hand. The features of this model, which is almost as simple and fast as Hillas' algorithm, turn out to be surprisingly close to the interaction model in HEMAS. Because it is tuned to fixed target data for $E_{\rm Lab} \leq 1$ TeV, it can supplement high energy models such as HEMAS and SIBYLL at low energy. The model contains about 10% of projectile diffraction dissociation.

HEMAS. The model of Forti et al.[36] is based on the UA5 Monte Carlo [40] generalized [41] for nuclear targets. Particles are produced in clusters with a distribution tuned to reproduce the observed multiplicity distribution and rapidity distribution in the central region ($|\eta| < 5$) for energies $53 < \sqrt{s} < 900$ GeV. This model also contains about 10% of projectile diffraction dissociation.

SIBYLL. The goal of this work [42] is to construct a Monte Carlo for cascade simulation in which many detailed features follow from an underlying physical model. At low energies, the algorithm is close to the Lund Monte Carlo PYTHIA [43], based on the dual parton model of Capella *et al.* [44], but tuned primarily to the fragmentation region, as is appropriate for a cascade calculation. The algorithm differs technically from PYTHIA in that it is designed to work efficiently when called with a random sequence of interaction energies and projectiles. At high energies (above $\sqrt{s} \sim 50$ GeV) minijet production becomes important. The rate at which production of minijets (i.e. QCD jets of only a few GeV) increases with energy is related to the rise of the cross section in an eikonal model.[45, 46] This model also contains somewhat less than 10% projectile dissociation events, but the amount and energy dependence of diffraction dissociation is a source of uncertainty in all the models.

Characteristic output of the various models for p-air interactions is summarized in Tables 2-6.

Uncertainty in transverse momentum distribution leads directly to an uncertainty in lateral distribution of muons in a cascade. It turns out that this is the largest source of uncertainty arising from the interaction model, so it deserves some comment. The transverse momentum distribution for forward pions is dominated by the most numerous secondaries of relatively low energy (i.e. by the central region). HEMAS and SIBYLL

Table 3: Mean p_T (charged secondaries).

E_{lab}(TeV)	NIM85	TARGET	HEMAS	SIBYLL
1	0.27	0.35	0.38	0.34
10	0.26	0.37	0.40	0.35
100	0.26	0.40	0.45	0.36
1000	0.26	0.43	0.50	0.38

Table 4: Fractional momentum of leading nucleon.

E_{lab}(TeV)	NIM85	TARGET	HEMAS	SIBYLL
1	0.51	0.45	0.41	0.44
10	0.51	0.44	0.40	0.44
100	0.50	0.43	0.42	0.42
1000	0.50	0.43	0.42	0.41

Table 5: Total fractional momentum of $\pi^{\pm}$ ($K^{\pm}$).

E_{lab}(TeV)	NIM85	TARGET	HEMAS	SIBYLL
1	0.29 (0.030)	0.31 (0.047)	0.27 (0.032)	0.26 (0.036)
10	0.29 (0.032)	0.33 (0.044)	0.29 (0.039)	0.27 (0.039)
100	0.30 (0.032)	0.35 (0.038)	0.29 (0.042)	0.28 (0.043)
1000	0.29 (0.033)	0.35 (0.035)	0.29 (0.046)	0.29 (0.043)

Table 6: Ratio $K^{\pm}$ to $K^{\pm} + \pi^{\pm}$.

E_{lab}(TeV)	NIM85	TARGET	HEMAS	SIBYLL
1	0.073	0.101	0.070	0.086
10	0.080	0.103	0.075	0.096
100	0.084	0.103	0.082	0.101
1000	0.089	0.103	0.089	0.102

are tuned to reproduce the distribution in that kinematic region. The NIM85 model is a pure scaling model with transverse momentum distribution tuned to data at 30 GeV beam energy. At that low energy, the overall average transverse momentum of charged pions is $\langle p_T \rangle \approx 0.33$ GeV/c, with a seagull effect as shown in Fig. 2. As energy increases, $\langle p_T \rangle$ becomes dominated by the increasing number of particles at low x. Therefore, because the transverse momentum distribution as a function of Feynman x is energy independent in the NIM85 model, the overall average transverse momentum becomes artificially low at high energy, as indicated by the entries in Table 3.

The other three models all have $\langle p_T \rangle$ increasing with energy, as required by collider data in the central region. In addition, in the HEMAS model, the transverse momentum is increased relative to that for pp interactions based on the results of Cronin et al.[47] In HEMAS, both of the effects that increase transverse momentum are superimposed on the seagull effect, with the result shown by the dashed line in Fig. 2. The concatenation of three effects (increase of $\langle p_T \rangle$ with energy, increase due to nuclear target and the "seagull" effect) is a conjecture that may well overestimate the transverse momentum of energetic secondaries.

Note that SIBYLL is intermediate–closer to HEMAS at low x to agree with collider data in the central region and close to NIM85 at high x This is because the physical origin of increasing transverse momentum in SIBYLL (minijets) operates only in the central region. The physical origin of the seagull effect in this model is separate. It arises from a higher transverse momentum for the diquark fragment of the proton, which then leads to higher p_T for pions radiated by the diquark, which populate the fragmentation region.

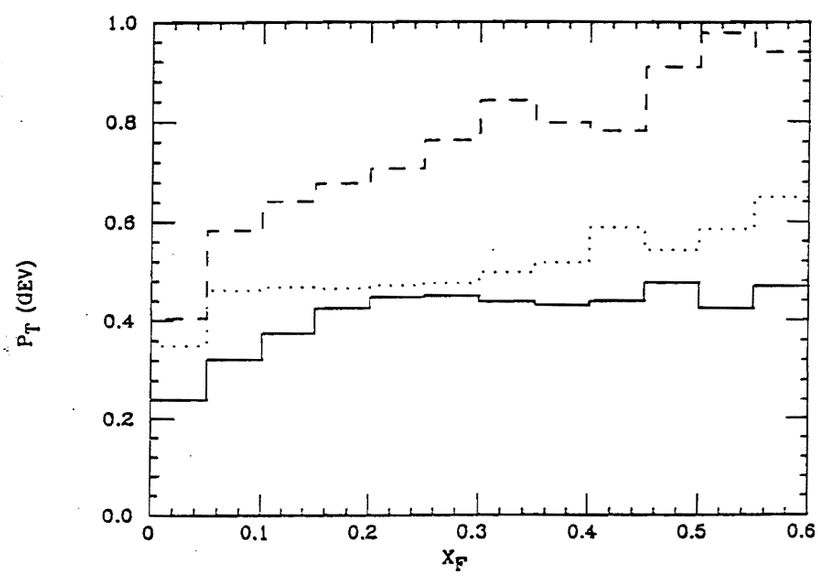

Fig. 2. Mean p_T *versus* Feynman x for charged secondaries at $E_{\rm Lab} = 100$ TeV.

Table 7: N_μ, $\langle r \rangle$ in m, $\langle r^2 \rangle$ in m^2, $\langle h \rangle_\mu$ in km.

$E_{\rm lab}$(TeV)		NIM85	TARGET	HEMAS	SIBYLL
	$\langle N_\mu \rangle$	0.66	0.64	0.67	0.59
100	$\langle r \rangle$	3.1	5.3	5.6	4.7
	$\langle r^2 \rangle$	18	51	65	62
	$\langle h \rangle$	15.1	16.8	16.8	–
	$\langle N_\mu \rangle$	3.51	3.71	3.61	3.79±.08
1000	$\langle r \rangle$	2.3	3.9	4.0	3.22±.06
	$\langle r^2 \rangle$	12	28	37	24
	$\langle h \rangle$	11.3	13.4	13.3	13.3

3.3 High energy muons in showers

To explore the effects of uncertainties of various aspects of the physical properties of hadronic interactions, I compare the number and lateral distributions of high energy muons in showers simulated with these four models. The comparison is made in the atmosphere to avoid any uncertainty associated with propagation through the rock. Table 7 summarizes some results for muons with $E_\mu > 1$ TeV at 2000 m.a.s.l. in the atmosphere.

All the models give similar results for $\langle N_\mu \rangle$ as a function of energy, but with $\sim 25\%$ higher normalization than the parametrizations. This is because the parametrizations give the mean number of muons at the depth of a detector. In the formulas of Refs. [38, 36] E_μ is not the energy of the muon at the surface, but only a parametric representation of the dependence on slant depth of rock.

Note that the height of origin of the muons reflects primary energy and causes an inverse relation between lateral spread and primary energy. Higher energy showers have to develop further to reach a given pion energy; hence muons of a given energy are more compact in higher energy showers. The distribution of height of origin has a broad tail at high altitude, which leads to a relatively flat lateral distribution. This is true independently of whether the p_T-distribution has a high-p_T tail.

A remarkable feature is the similarity of $\langle N_\mu \rangle$ in the NIM85 model to the others despite the large difference in multiplicity of muons in single interactions. Understanding this fact is actually quite instructive. Energy conservation forces the lower multiplicity model to have a harder Feynman x distribution for the pions. The multiplicity for HEMAS is 50% larger, but the NIM85 distribution is harder and exceeds the inclusive pion distribution of HEMAS for $\eta > 5$. With the harder secondary pion distribution, muons of a given energy can be produced by lower energy interactions, which are more numerous in the cascade. This illustrates a common occurence in cascade calculations: a change in the interaction model leads to only a second order change in the cascade.

Unfortunately, this is not the case for $\langle p_T \rangle$. Any uncertainty in transverse momentum

shows up directly as a corresponding uncertainty in the lateral distribution. The different values of $\langle r \rangle$ and $\langle r^2 \rangle$ in Table 7 reflect the difference in $\langle p_T \rangle$ discussed in the previous subsection.

4 Conclusion

Parametrizations of multiplicity and lateral distribution of deep underground muons have clearly been useful in obtaining a preliminary understanding of the data.[28, 30, 29, 24, 49, 50] However, their use has important limitations associated with omission of certain correlations that must be present at some level. One such effect due to nuclear projectiles was discussed here in §3.1. In addition, correlations in lateral structure of high multiplicity events are to be expected from jet production in high energy interactions. One also expects [48] an anti-correlation between number of muons underground and shower size at the surface because more energy into muons at high altitude should be associated with a more rapidly developing, somewhat smaller electromagnetic shower. As discussed here in §3.2 and §3.3, there is also considerable uncertainty in the treatment of transverse momentum dependence of hadronic/nuclear interactions at high energy. To some extent the corresponding uncertainty in lateral distribution can be dealt with experimentally by measuring it, but there remains a complication due to the fact that both the primary composition and the model of hadronic interactions affect the lateral distribution.

For these reasons, conclusions about primary spectrum based on use of parametrizations to interpret underground muon data must be considered tentative and preliminary. Analyses of data from most of the deep underground experiments suggest a relatively "light" composition in the region of the knee, which still includes, however, a significant fraction ($\gtrsim$ 20%) of heavy nuclei when compared by energy per nucleus. It is interesting (though dangerous) to speculate on what changes in interpretation might result from a realistic treatment of the various physical processes, such as nuclear fragmentation and jet production, with a full Monte Carlo. On the one hand, the transverse momentum distribution in the HEMAS hadron-nucleus model is probably overestimated on average. On the other, realistic treatment of nuclear fragmentation will lead to broader lateral distribution of high multiplicity events; that is, heavy nuclei will look somewhat more proton-like.

Use of constraints from other kinds of air shower experiments, as discussed here in §2, as well as normalization of trial compositions to all existing direct measurements is needed to reach a firm conclusion. Observation of air showers at the surface in coincidence with deep underground muons [51, 50] is of particular interest.[52] The prospect of extending direct measurements up to 10^{15} eV [53, 54], which is the subject of the GOAL initiative, should provide the basis for a definitive understanding of the relative importance of various groups of nuclei in the region of the knee of the spectrum.

ACKNOWLEDGEMENTS. I am grateful to Paolo Lipari and Todor Stanev for discussions on many aspects of this talk.

References

[1] Peters, B. 1959, *Nuovo Cimento (Suppl)*, **14**, 436 and *Nuovo Cimento* **22**, 800 (1961).

[2] Ginzburg, V.I. and Syrovatskii, S.I., 1964. *The Origin of Cosmic Rays* (Pergamon Press).

[3] Krimsky, G.F. 1977, *Dokl. Akad. Nauk SSSR*, **243**, 1306.

[4] Axford, W.I., Leer, E. and Skadron, G. 1977, in *Proc. 15th Int. Cosmic Ray Conf. Plovdiv, Bulgaria* (Bulgarian Academy of Sciences, 1977) **11**, 132.

[5] Bell, A.R. 1978, *M.N.R.A.S.* **182**, 147 and 443.

[6] Blandford, R.D. and Ostriker, J.P., 1978. *Astrophys. J.* **221**, L29.

[7] Lagage, P.O. and Cesarsky, C.J. 1983, *Astron. Astrophys.* **118**, 223 and **125**, 249.

[8] Jokipii, J.R. 1987. *Ap. J.,* **313**, 842. See also *Proc. 6th Intl. Solar Wind Conf.,* **II**, 481, Estes Park, CO.

[9] Völk, H.J. and Biermann, P.L. 1988, *Ap. J. Lett.* **333**,

[10] Ip, W.H. and Axford, W.I. 1992, in *Particle Acceleration in Cosmic Plasmas*, ed.'s G.P. Zank and T.K. Gaisser, AIP, in press.

[11] Jokipii, J.R. and Morfill, G. 1991 in *Astrophysical Aspects of the Most Energetic Cosmic Rays*, eds. M. Nagano and F. Takahara, (World Scientific, Singapore, 1991) p. 261 and earlier references therein.

[12] Wdowczyk, J.and Wolfendale, A.W. 1989, *Ann. Rev. Nucl. Part. Sci.* **39** 43.

[13] Fichtel, C.E. and Linsley, J. 1986 *Ap. J.* **300**, 474.

[14] Protheroe, R.J. and Szabo, A.P., *Phys. Rev. Letters* **69**, 2885 (1992).

[15] Gaisser, T.K., Stanev, T. and Zank, G., 1992 (in preparation).

[16] Nagano, M. *et al.* 1984. *J. Phys G*, **10**, 1295.

[17] Fomin, Yu.A., *et al.*, 1991. *Proc. 22nd International Cosmic Ray Conf.* (Dublin) **2**, 85.

[18] Asakimori, K. *et al.* in *Proc. 22nd Int. Cosmic Ray Conf, Dublin, Ireland* (Dublin Institute for Advanced Studies, Dublin, Ireland, 1991) **2** 57-60 and 97-100.

[19] Grigorov, N.L. *et al.* 1971, in *Proc 12th Int. Cosmic Ray Conf. Hobart, Tasmania* (Univ. of Tasmania Press, Hobart, Tasmania, 1971) **2** 206.

[20] Engelmann, J.J. *et al.* 1990, *Astron. Astrophys.,* **233**, 96.

[21] Swordy, S.P. *et al.* 1990, *Ap. J.* **349**, 625 and Müller, D. *et al.* 1991, *Ap. J.* **374**, 356.

[22] Ellsworth, R.W. *et al.* 1977. *Astrophys. Space Sci.* **52**, 415.

[23] Gaisser, T.K. 1990. In *Astrophysical Aspects of the Most Energetic Cosmic Rays* (ed. M. Nagano & F. Takahara, World Scientific) p. 146.

[24] Aglietta, M. *et al.* 1989. In *Proc. Topical Seminar on Astrophysics and Particle Physics*, San Miniato, Italy *Nucl. Phys.* **14B**, 193 (1990).

[25] R. Ren *et al.* 1988. *Phys. Rev.* **D38**, 1404.

[26] G.B. Yodh *et al.* 1984. *Phys. Rev.* **D29**, 892.

[27] J. Kempa & J. Wdowczyk 1983. *J. Phys.* **G9**, 1271.

[28] Cebula, D. *et al.*, 1990. *Ap. J.* **358**, 637.

[29] Auriemma, G., Bussino, S., Gaisser, T.K. and Stanev, T., 1991. *Proc. 22nd Int. Cosmic Ray Conf.* (Dublin) **2**, 101.

[30] Ahlen, S. *et al.* (MACRO Collaboration), 1992. *Phys. Rev. D* **46**, 895.

[31] Chatelet, E. *et al.*, 1991. *Proc. 22nd International Cosmic Ray Conf.* (Dublin) **2**, 45.

[32] Erlykin, A.D. 1992. These Proceedings.

[33] Gaisser, T.K. et al., 1992. Submitted to Phys. Rev. D.

[34] Gaisser, T.K. 1992. To appear in Proc. Paris Workshop on Techniques to Study Cosmic Rays (ed. J.W. Cronin & A.A. Watson, Nuclear Physics B, Proc. Supp.)

[35] Engel, J., Gaisser, T.K., Lipari, P., and Stanev, T., 1992. *Physical Review D* (to be published).

[36] Forti, C. *et al.* 1990. *Phys. Rev.* **D42**, 3668.

[37] Hillas, A.M., 1981. *Proc. 17th Int. Cosmic Ray Conf.* (Paris) vol. 8, p. 193.

[38] Gaisser, T.K. & Stanev, T., 1985. *Nuclear Instruments & Methods* **A235**, 183.

[39] Barr, G., Gaisser, T.K. & Stanev, T., 1989. *Phys. Rev.* **D39**, 3532.

[40] Alner, G.J. *et al.*, 1986. Report No. CERN-EP/86/213 and *Physics Lett.* **167B**, 476.

[41] Forti, Carlo, 1988. Tesi di Laurea, Università di Roma I.

[42] Lipari, P., Fletcher, R.S., Gaisser, T.K. and Stanev, T., 1991. *Proc. 22nd Int. Cosmic Ray Conf.* (Dublin) 4, 197.

[43] Bengtsson, H. & Sjöstrand, T., 1987. *Comp. Phys. Comm.* **46**, 43.

[44] Capella, A. & Tran Thang Van, J., 1981. *A. Phys.* **C10**, 249.

[45] Durand, L. & Pi, H., 1987. *Phys. Rev. Letters* **58**, 303.

[46] Gaisser, T.K. & Stanev, T., 1989. *Physics Lett.* **B219**, 375.

[47] Cronin, J.W., *et al.*, 1975. *Phys. Rev.* **D11**, 3105.

[48] Bilokon, H. *et al.*, 1990. *Proc. 21st Int. Cosmic Ray Conf.* (Adelaide) vol. 9, p. 114.

[49] Chudakov, A.E., Tsyabuk, A.L., & Voevodsky, A.V., 1991. *Proc. 22nd Int. Cosmic Ray Conf.* (Dublin) vol. 2, p. 5.

[50] Das Gupta, U., Fields, T.H. & Ruddick, K., 1991. *Proc. 22nd Int. Cosmic Ray Conf.* (Dublin) vol. 2, p. 33.

[51] Bellotti, R. *et al.*, 1990. *Phys. Rev.* **D42**, 1396.

[52] Gaisser, T.K., Lipari, P. & Stanev, T., 1990. *Proc. 21st Int. Cosmic Ray Conf.* (Adelaide) vol. 9, p. 232.

[53] Forman, M.A. *et al.* 1992. To appear in the *Proc. VII Int. Symp. on Very High Energy Cosmic Ray Interactions* (Ann Arbor, June 1992).

[54] Müller, D., 1992. These Proceedings.